

## Local-field factors in a polarized two-dimensional electron gas

Juana Moreno and D. C. Marinescu

*Department of Physics, Clemson University, Clemson, South Carolina 29634, USA*

(Received 4 June 2002; revised manuscript received 15 November 2002; published 26 November 2003)

We derive approximate expressions for the static local-field factors of a spin-polarized two-dimensional electron gas that smoothly interpolate between their small- and large-wave-vector asymptotic limits. The proposed analytical expressions reproduce recent diffusion Monte Carlo data for the unpolarized and fully polarized electron gas. We find that the degree of spin polarization produces important modifications to the local factors of the minority spins, while the local-field functions of the majority spins are less affected.

DOI: 10.1103/PhysRevB.68.195210

PACS number(s): 71.10.-w, 72.25.-b, 71.45.Gm, 75.50.Pp

### I. INTRODUCTION

Most many-body theories of electronic systems regard the spin polarization as a small parameter. This picture is certainly true when the Zeeman splitting is much smaller than other relevant energies in the problem. Recently, however, attention has been focused on materials in which the Zeeman splitting dominates the energy spectrum, such as diluted magnetic semiconductors. The large Zeeman splitting is due to the strong exchange interactions between the itinerant carriers and the magnetic ions that generate a value of the effective gyromagnetic factor  $\gamma^*$  up to hundreds of times its band value. As a consequence, even in weak magnetic fields these systems can be fully polarized.<sup>1</sup> Due to their easy polarizability, the diluted magnetic semiconductors are promising candidates to be used in spin-dependent conduction in solid-state devices;<sup>2</sup> hence the interest in developing a correct microscopic model for them.

In this paper, we examine the short-range effects of the Coulomb interaction in a two-dimensional polarized electron gas. A realistic picture of the spin-polarized electron gas hinges on finding an appropriate description of the many-body interaction, which has to incorporate the explicit spin dependence of the short-range Coulomb repulsion. The self-consistent treatment of the exchange and correlation effects has proven to be very important in understanding the physics of normal metals,<sup>3</sup> but to our knowledge it has not been fully analyzed in spin-polarized systems. In addition, the relevance of the exchange and correlation effects increases as the dimensionality of the electron gas is lowered.

We model the exchange and correlation hole around each electron by using spin-dependent local-field correction functions  $\tilde{G}_\sigma^\pm(\mathbf{q}, \omega)$ .<sup>4-7</sup> An additional local-field factor ( $G_\sigma^n$ ) is needed to relate the interacting polarization function (zero-order term in the diagrammatic expansion of the charge-charge correlation function)  $\Pi_{\sigma\sigma}$  with the noninteracting one  $\Pi_{\sigma\sigma}^0$  as in Ref. 8

$$\Pi_{\sigma\sigma}(\mathbf{q}, \omega) = \frac{\Pi_{\sigma\sigma}^0(\mathbf{q}, \omega)}{1 + 2v(\mathbf{q})G_\sigma^n(\mathbf{q}, \omega)\Pi_{\sigma\sigma}^0(\mathbf{q}, \omega)}. \quad (1)$$

This parametrization of the modified polarization function leads to a renormalized expression of the local fields that determine the response functions, so that the complete local-

field functions are given as  $G_\sigma^\pm = \tilde{G}_\sigma^\pm + G_\sigma^n$ .<sup>8</sup> In an unpolarized electron gas,  $G^+ = G_\uparrow^+ = G_\downarrow^+$  appears only in the expressions of the electrical response functions, and  $G^- = G_\uparrow^- = G_\downarrow^-$  only in the magnetic response susceptibilities. However, in a polarized electron system the four local-field factors appear in all the response functions.

The determination of the frequency and wave-vector dependence of the local-field corrections is a very difficult problem which remains unsolved even in the case of the unpolarized electron system. Fortunately, the asymptotic values of the local-field factors can be obtained exactly in some limit cases.<sup>7,9,10</sup> Numerical estimates of the response functions of the two- and three-dimensional unpolarized electron gas have shown that local-field factors smoothly interpolate between the asymptotic small- and large-wave-vector behavior.<sup>11</sup> This feature is expected to exist also in the case of a spin-polarized system. Consequently, we use the asymptotic limits of the static local factors for large and small wave vector as a starting point in deriving their approximate expressions across the whole spectrum of momentum.

The fundamental parameters of the problem are the coupling strength  $r_s = a_B^*/\sqrt{\pi(n_\uparrow + n_\downarrow)} = a_B^*/\sqrt{\pi n}$  (Ref. 12) and the spin polarization  $\zeta = (n_\uparrow - n_\downarrow)/n$ . Since the many-body interaction is independent of the source of the polarization, we expect our results to maintain their validity also in the case of an itinerant ferromagnet with a self-induced magnetic field, or when the polarization is achieved by other means, such as shining circularly polarized light on the sample.

In Sec. II, we study the large- and small-wave-vector limits of the local-field functions and their dependence with the electronic density and polarization. In Sec. III, we give a simple parametrization of the local-field factors that satisfy the asymptotic limits and reproduces the most recent numerical results for the unpolarized and fully polarized electron gas.<sup>11</sup> Section IV presents our conclusions.

### II. LIMITING BEHAVIOR OF THE LOCAL-FIELD FACTORS

#### A. Small wave vector

At zero frequency and small wave vector, sum rules are used to connect the static limits of various response functions to certain thermodynamic coefficients, which can be ex-

pressed as derivatives of the ground-state energy of the electron gas.<sup>9</sup> Subsequently, the renormalized local-field functions, which are directly connected with these response functions, are written down as derivatives of the exchange and correlation energy of the interacting electron gas ( $E^{xc}$ ):

$$G_{\sigma}^{+}(\mathbf{q}\rightarrow 0) = \frac{\tilde{q}r_s^2}{8\sqrt{2}} \left( \frac{\partial \epsilon^{xc}}{\partial r_s} - r_s \frac{\partial^2 \epsilon^{xc}}{\partial r_s^2} + 2 \operatorname{sgn}(\sigma) \frac{\partial^2 \epsilon^{xc}}{\partial r_s \partial \zeta} \right), \quad (2)$$

$$G_{\sigma}^{-}(\mathbf{q}\rightarrow 0) = \frac{\tilde{q}r_s}{2\sqrt{2}} \left( -\frac{\partial^2 \epsilon^{xc}}{\partial \zeta^2} + \operatorname{sgn}(\sigma) \frac{r_s}{2} \frac{\partial^2 \epsilon^{xc}}{\partial r_s \partial \zeta} \right), \quad (3)$$

where  $\tilde{q} = \mathbf{q}/k_F$  is the normalized momentum,  $\epsilon^{xc} = E^{xc}/N$  is the exchange and correlation energy per particle measured in rydbergs and the coupling strength  $r_s$  is measured in units of the effective Bohr radius of the system.<sup>12</sup> Using the explicit expression of the exchange energy the local-field functions become

$$G_{\uparrow}^{+}(\mathbf{q}\rightarrow 0) = \frac{\tilde{q}}{2\pi} [(2+\zeta)\sqrt{1+\zeta} - \zeta\sqrt{1-\zeta}] + \frac{\tilde{q}r_s^2}{8\sqrt{2}} \left( \frac{\partial \epsilon^c}{\partial r_s} - r_s \frac{\partial^2 \epsilon^c}{\partial r_s^2} + 2 \frac{\partial^2 \epsilon^c}{\partial r_s \partial \zeta} \right), \quad (4)$$

$$G_{\uparrow}^{-}(\mathbf{q}\rightarrow 0) = \frac{\tilde{q}}{2\pi} \left( \frac{2+\zeta}{\sqrt{1+\zeta}} + \frac{\zeta}{\sqrt{1-\zeta}} \right) + \frac{\tilde{q}r_s}{2\sqrt{2}} \left( -\frac{\partial^2 \epsilon^c}{\partial \zeta^2} + \frac{r_s}{2} \frac{\partial^2 \epsilon^c}{\partial r_s \partial \zeta} \right). \quad (5)$$

Similar expressions apply to  $G_{\downarrow}^{\pm}$  due to the fact that  $G_{\downarrow}^{\pm}(\zeta) = G_{\uparrow}^{\pm}(-\zeta)$ .

The inclusion of the correlation energy in the small  $\mathbf{q}$  limit of the local-field factors is crucial to correctly evaluate the response functions. If only the exchange contribution to the local-field factors is included, the magnetic susceptibility of the unpolarized gas develops a pole for  $r_s \geq \pi/\sqrt{2} \sim 2.221$ ,<sup>13</sup> in disagreement with the results of extensive numerical calculations that show a stable paramagnetic phase up to  $r_s \lesssim 26$ .<sup>14,15</sup>

To precisely evaluate the contribution from the correlation energy to  $G_{\sigma}^{\pm}(\mathbf{q}\rightarrow 0)$  we use the latest numerical computation of the ground-state energy of the two-dimensional electron gas by Attacalite *et al.*<sup>15</sup> By taking the appropriate derivatives of Eq. (3) in Ref. 15, we derive analytical expressions for the initial slope of the static local-field correction functions:  $\alpha_{\sigma}^{\pm} = G_{\sigma}^{\pm}(\tilde{q}\rightarrow 0)/\tilde{q}$ .

The behavior of  $\alpha_{\uparrow}^{+}(r_s, \zeta)$  and  $\alpha_{\uparrow}^{-}(r_s, \zeta)$  is quite different. Figure 1 shows  $\alpha_{\uparrow}^{+}(r_s, \zeta)$  as a function of the polarization for several values of  $r_s$ . Note that  $\alpha_{\uparrow}^{+}$  is always positive, as the local effects always decrease the uniform electron density at large interelectronic distances. Also note that  $\alpha_{\uparrow}^{+}$  for small values of  $r_s$  is a monotonically increasing function of  $\zeta$ . This behavior can be understood by analyzing the contri-

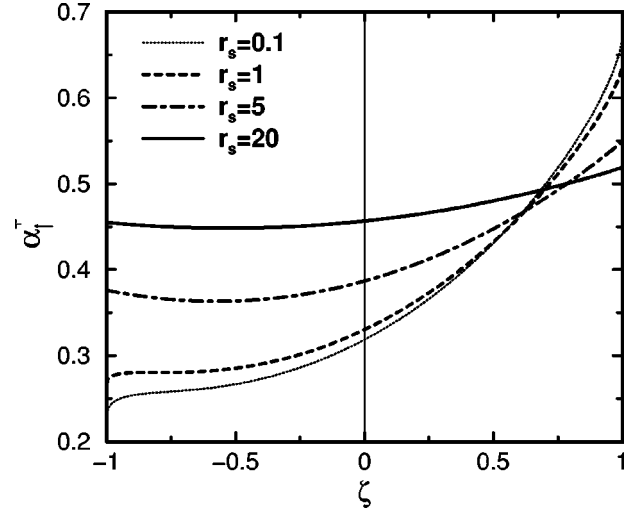


FIG. 1. Initial slope  $\alpha_{\uparrow}^{+}(r_s, \zeta)$  of the local-field factor as a function of the polarization  $\zeta$  for  $r_s=0.1$  (dotted curve),  $r_s=1.0$  (dashed curve),  $r_s=5.0$  (dot-dashed curve), and  $r_s=20.0$  (solid curve).

bution from the exchange interaction, which dominates at large electronic densities, given by  $\alpha_x^{+} = [(2+\zeta)\sqrt{1+\zeta} - \zeta\sqrt{1-\zeta}]/2\pi$ . Since the exchange interaction takes place only between electrons with parallel spin, increasing values of  $\zeta$  induce larger effects and further reduction of the uniform electron density at small  $\mathbf{q}$ . Consequently, the value of  $\alpha_{\uparrow}^{+}$  increases. Correlation effects become more important with increasing  $r_s$  and they partly cancel the strong  $\zeta$  dependence of  $\alpha_x^{+}$ , as it can be seen in Fig. 1.

Figure 2 displays  $\alpha_{\uparrow}^{+}(r_s, \zeta)$  as a function of  $r_s$  for different values of the spin polarization. It can be noted that  $\alpha_{\uparrow}^{+}$  is a monotonic increasing function of  $r_s$  for values of  $\zeta \lesssim 0.5$ . This feature is also displayed in Fig. 1. In particular, as pre-

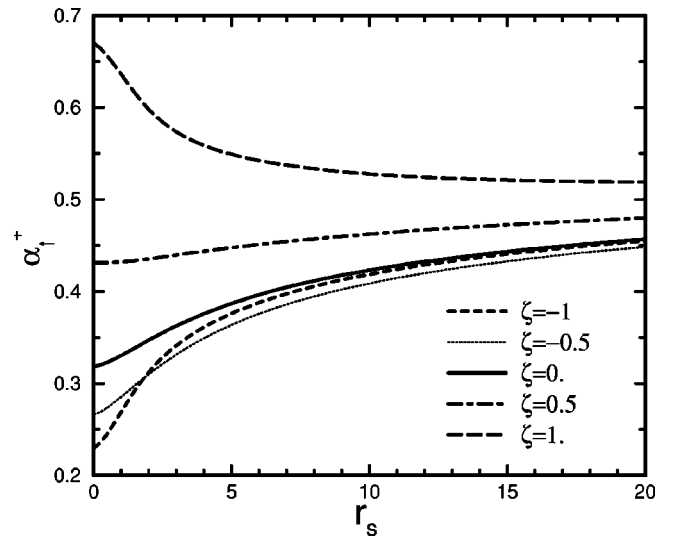


FIG. 2. Initial slope  $\alpha_{\uparrow}^{+}(r_s, \zeta)$  of the local-field correction as a function of the coupling strength  $r_s$  for different values of the spin polarization:  $\zeta=-1$  (dashed curve),  $\zeta=-0.5$  (dotted curve),  $\zeta=0.0$  (solid curve),  $\zeta=0.5$  (dot-dashed curve), and  $\zeta=1$  (long-dashed curve).

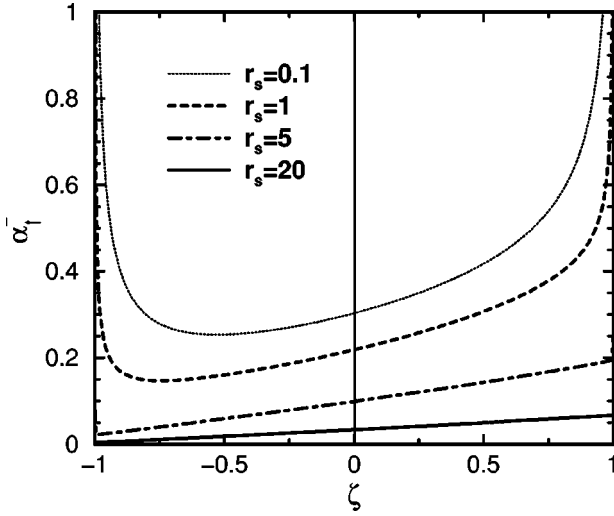


FIG. 3. Initial slope  $\alpha_{\uparrow}^{-}(r_s, \zeta)$  of the local-field factor as a function of the polarization for different values of  $r_s$  as indicated in the legend.

viously noticed,<sup>11</sup> in the unpolarized electron gas  $\alpha_{\uparrow}^{+}(r_s, \zeta = 0)$  increases with  $r_s$ .

Figure 3 displays the initial slope  $\alpha_{\uparrow}^{-}(r_s, \zeta)$  as a function of  $\zeta$  for different values of  $r_s$ . As in the case of  $\alpha_{\uparrow}^{+}$ , the main contribution for small values of  $r_s$  came from the exchange energy:

$$\alpha_x^{-} = \frac{1}{2\pi} \left( \frac{2+\zeta}{\sqrt{1+\zeta}} + \frac{\zeta}{\sqrt{1-\zeta}} \right).$$

For large electronic densities  $\alpha_{\uparrow}^{-}$  diverges for a fully polarized system ( $\zeta = \pm 1$ ), behavior explained by the fact that in a fully polarized gas the magnetic susceptibility becomes zero. As  $r_s$  increases, correlation effects quench by an exponential factor the diverging contribution from the exchange energy.<sup>16</sup> Thus, correlation effects become dominant at small densities and the strong dependence of  $\alpha_{\uparrow}^{-}$  on  $\zeta$  is completely washed out. Instead, at large values of  $r_s$ ,  $\alpha_{\uparrow}^{-}$  becomes a linear function of  $\zeta$ .

Figure 4 displays  $\alpha_{\uparrow}^{-}(r_s, \zeta)$  as a function of  $r_s$  for different values of the spin polarization. The divergence at  $r_s = 0$  and  $\zeta = \pm 1$  is clearly displayed. Note that  $\alpha_{\uparrow}^{-}$  is a monotonic decreasing function of  $r_s$  for any value of  $\zeta$ .

### B. Large wave vector

In the limit of large wave vector it is easier to derive independently expressions for  $\tilde{G}_{\sigma}^{\pm}$  and for  $G_{\sigma}^n$ . For large frequency or large wave vector, an iterative method generates the exact asymptotic expressions for  $\tilde{G}_{\sigma}^{\pm}$ .<sup>17</sup> For a two-dimensional electron gas,<sup>10</sup>

$$\tilde{G}_{\uparrow}^{+}(\mathbf{q} \rightarrow \infty) = \beta_{\uparrow}^{+}(r_s, \zeta) = 1 - \frac{1}{2} g_{\uparrow\downarrow}(0), \quad (6)$$

$$\tilde{G}_{\uparrow}^{-}(\mathbf{q} \rightarrow \infty) = \beta_{\uparrow}^{-}(r_s, \zeta) = \frac{1}{2} g_{\uparrow\downarrow}(0), \quad (7)$$

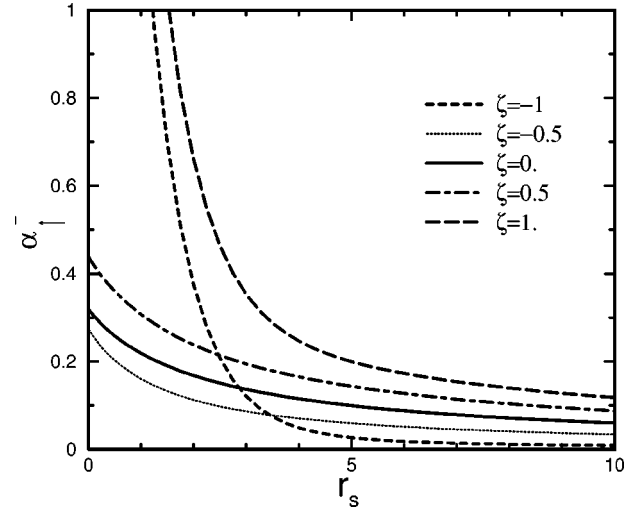


FIG. 4. Initial slope  $\alpha_{\uparrow}^{-}(r_s, \zeta)$  as a function of  $r_s$  for different values of the spin polarization.

where  $g_{\uparrow\downarrow}(0)$  is the spin resolved pair-distribution function at the origin. It has been shown that  $g_{\uparrow\downarrow}(0)$  is largely unaffected by the degree of spin polarization.<sup>18,19</sup> In our calculation we use the simple expression  $g_{\uparrow\downarrow}(0) = 1/(1 + 0.6032 r_s + 0.07263 r_s^2)^2$ , where only the parameter  $r_s$  appears.<sup>19</sup> With this choice,  $\beta_{\uparrow}^{+}(r_s, \zeta) = \beta_{\downarrow}^{+}(r_s, \zeta) = \beta^{+}(r_s)$  and  $\beta_{\uparrow}^{-}(r_s, \zeta) = \beta_{\downarrow}^{-}(r_s, \zeta) = \beta^{-}(r_s)$ .

In order to calculate the large momentum behavior of  $G_{\sigma}^n$  we need to approximate the interacting polarization function,<sup>20,8</sup>

$$\Pi_{\sigma\sigma'}(\mathbf{q}, \omega) = \frac{1}{A} \sum_{\mathbf{k}} \frac{\bar{n}_{\mathbf{k},\sigma} - \bar{n}_{\mathbf{k}+\mathbf{q},\sigma'}}{\omega + \xi_{\mathbf{k}\sigma} - \xi_{\mathbf{k}+\mathbf{q}\sigma'}}, \quad (8)$$

where  $\xi_{\mathbf{k}\sigma} = \epsilon_{\mathbf{k}} + \text{sgn}(\sigma) \gamma^* B = k^2/2m + \text{sgn}(\sigma) \gamma^* B$  is the quasiparticle energy in the static magnetic field  $B$ ,  $\bar{n}_{\mathbf{k},\sigma}$  is the exact occupation number in the interacting electron gas, and  $A$  is the area of the system. Since at large  $\mathbf{q}$  the particle number renormalization is the dominant effect, Eq. (8) neglects the renormalization of the quasiparticle effective mass.

By making an asymptotic expansion of the interacting polarization function,<sup>20-22</sup> the local factor  $G_{\sigma}^n$  can be written down as

$$G_{\sigma}^n(\mathbf{q} \rightarrow \infty) = \frac{r_s}{\sqrt{2}} \frac{\Delta t_{\sigma}}{(1+\zeta)^2} \tilde{q} = \gamma_{\sigma}(r_s, \zeta) \tilde{q}, \quad (9)$$

where  $\tilde{q} = \mathbf{q}/k_F$  is the normalized momentum and  $\Delta t_{\sigma} = t_{\sigma} - t_{\sigma}^0$  is the difference between the kinetic energy of the electrons with spin  $\sigma$  in the interacting system,  $t_{\sigma} = (1/N) \sum_{\mathbf{k}} \bar{n}_{\mathbf{k}\sigma} (k^2/2m)$ , and in the noninteracting gas,  $t_{\sigma}^0 = (1/N) \sum_{\mathbf{k}} n_{\mathbf{k}\sigma}^0 (k^2/2m)$ , over the total number of electrons. This equation is valid when  $\Delta t_{\sigma}$  is measured in rydbergs and  $r_s$  in units of the effective Bohr radius.<sup>12</sup>

The difference in kinetic energies can be related with the exchange and correlation energies and their derivatives using the generalization of the virial theorem to polarized systems:<sup>23</sup>

$$\Delta t_\sigma = -\frac{1 + \text{sgn}(\sigma)\zeta}{2} \left[ \text{sgn}(\sigma) d \frac{\partial \epsilon^{xc}}{\partial \zeta} + r_s \frac{\partial \epsilon^{xc}}{\partial r_s} \right] - \epsilon_\sigma^{xc}, \quad (10)$$

where  $\epsilon_\sigma^{xc} = E_\sigma^{xc}/N$  is the average exchange and correlation energy of the electrons with spin  $\sigma$ .

The average exchange energy for any spin population is well known:  $\epsilon_\sigma^x = -(4\sqrt{2}/3\pi r_s)[1 + \text{sgn}(\sigma)\zeta]^{3/2}$  (Ry). The spin-dependent correlation energies are difficult to evaluate or to extract from numerical calculations. Therefore, we have to rely on same approximate scheme to extract the spin-dependent correlation energy from the available computations of the full correlation energy. The total correlation energy per particle is

$$\frac{E^c}{N} = \epsilon_\uparrow^c + \epsilon_\downarrow^c = \tilde{\epsilon}_\uparrow^c \frac{1 + \zeta}{2} + \tilde{\epsilon}_\downarrow^c \frac{1 - \zeta}{2}.$$

Perdew and Wang<sup>24</sup> suggested the following parametrization for the correlation energy of a polarized electron gas:

$$\epsilon^c(r_s, \zeta) = \epsilon^c(r_s, 0) + h(r_s, \zeta)f(\zeta), \quad (11)$$

where  $h(r_s, \zeta)$  is an even function of the polarization and

$$f(\zeta) = \frac{(1 + \zeta)^{3/2} + (1 - \zeta)^{3/2} - 2}{2(\sqrt{2} - 1)}$$

for a two-dimensional system.<sup>11</sup> This function can be decomposed as  $f(\zeta) = [f_\uparrow(\zeta)(1 + \zeta) + f_\downarrow(\zeta)(1 - \zeta)]/2$ , where  $f_\sigma = [\sqrt{1 + \text{sgn}(\sigma)\zeta} - 1]/(\sqrt{2} - 1)$ . An estimate of the spin-dependent correlation energies can be obtained as

$$\epsilon_\sigma^c(r_s, \zeta) = \frac{1 + \text{sgn}(\sigma)\zeta}{2} \tilde{\epsilon}_\sigma^c(r_s, \zeta),$$

where

$$\tilde{\epsilon}_\sigma^c(r_s, \zeta) = \epsilon^c(r_s, 0) + \frac{f_\sigma(\zeta)}{f(\zeta)} [\epsilon^c(r_s, \zeta) - \epsilon^c(r_s, 0)]. \quad (12)$$

Using the parametrization of the correlation energy proposed in Ref. 15 we obtain reasonable values for  $\epsilon_\sigma^c$ . Also, its dependence with the polarization is the expected one. At a fixed value of  $r_s$ ,  $\epsilon_\uparrow^c$  ( $\epsilon_\downarrow^c$ ) is a monotonic increasing (decreasing) function of  $\zeta$ .

Figure 5 shows the dependence of  $\gamma_\uparrow(r_s, \zeta)$ , Eq. (9), with the polarization for several values of  $r_s$ . While the initial slopes ( $\alpha_\sigma^\pm$ ) and the constant terms in the large  $\mathbf{q}$  limit ( $\beta^\pm$ ) of the local factors are always positive, the coefficient  $\gamma_\sigma$  can have any sign. Since  $\gamma_\sigma \propto \Delta t_\sigma$ , a change in sign of  $\gamma_\sigma$  implies a change of sign of  $\Delta t_\sigma = t_\sigma - t_\sigma^0$ . Even though, for a given spin  $\Delta t_\sigma$  can be negative, we have checked that the difference in the total kinetic energies of the interacting and the noninteracting system,  $\Delta T = N(\Delta t_\uparrow + \Delta t_\downarrow)$ , is positive for any value of  $\zeta$  and  $r_s$ .<sup>20</sup>

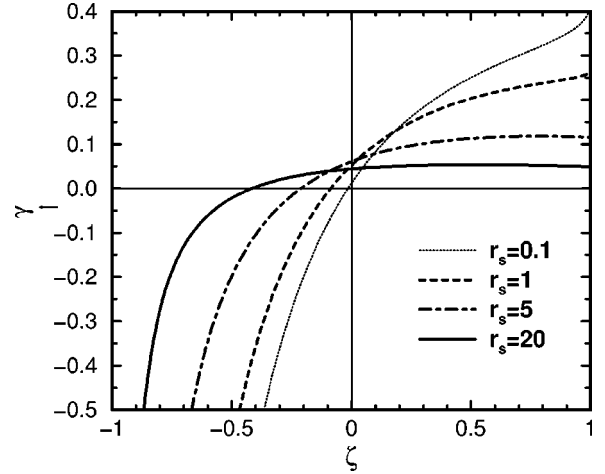


FIG. 5. The coefficient  $\gamma_\uparrow(r_s, \zeta)$  as a function of  $\zeta$  for different values of  $r_s$  as indicated in the legend.

The negative value of  $\Delta t_\uparrow$  for negative polarizations is easily understood if the variation with the polarization of the carrier effective mass is considered. It is well known that in a polarized electron gas the mass of the minority- (majority-) spin populations increases (decreases) with the value of the polarization.<sup>25</sup> Therefore, for large enough values of  $\zeta$  the mass renormalization dominates, and the kinetic energy of the minority (majority) carriers is reduced (increased) with respect to its free-electron value. Also, as  $\zeta$  increases, the exchange effects between the minority (majority) spins are greatly reduced (increased). Due to the combination of these two effects the electrons from the majority-spin population will tend to accumulate around the few minority spins increasing the local charge around them. This generates a negative value of  $G^n(\mathbf{q} \rightarrow \infty)$  for the minority spins. The opposite is true for the majority spins.

At small values of  $r_s$  and finite values of the polarization, the kinetic energy of each spin population is dominated by the exchange contribution,  $\Delta t_\sigma \sim \zeta/r_s$ , a behavior that is independent of the parametrization used to obtain the spin-dependent correlation energy, Eq. (12) in our case. At large values of  $r_s$ , the correlation effects become more important as it can be seen in Fig. 5. Finally, we point out that the large effect of the polarization in the value of  $\gamma_\uparrow(r_s, \zeta)$  is mainly due to the denominator  $(1 + \zeta)^2$  of Eq. (9).

Figure 6 displays  $\gamma_\uparrow(r_s, \zeta)$  as a function of  $r_s$  for several values of  $\zeta$  between  $\zeta = -0.75$  and  $\zeta = 1$ . The same trends as in Fig. 5 become apparent. For the unpolarized electron gas  $\gamma_\uparrow$  increases with  $r_s$ , reaches a maximum at  $r_s = 2.88$ , and decreases afterwards. For  $\zeta = 1$ ,  $\gamma_\uparrow$  monotonically decreases with  $r_s$ .

### III. SPIN-DEPENDENT LOCAL-FIELD CORRECTIONS

Numerous parametrized expressions of the local-field factors for the unpolarized three-dimensional<sup>26,27,5,28</sup> and two-dimensional<sup>29,30,21</sup> electron gas have been suggested since the pioneering work of Hubbard.<sup>31</sup> However, parametrized expressions of  $G^\pm$  for the polarized gas have not received so much attention. Numerical calculations in the

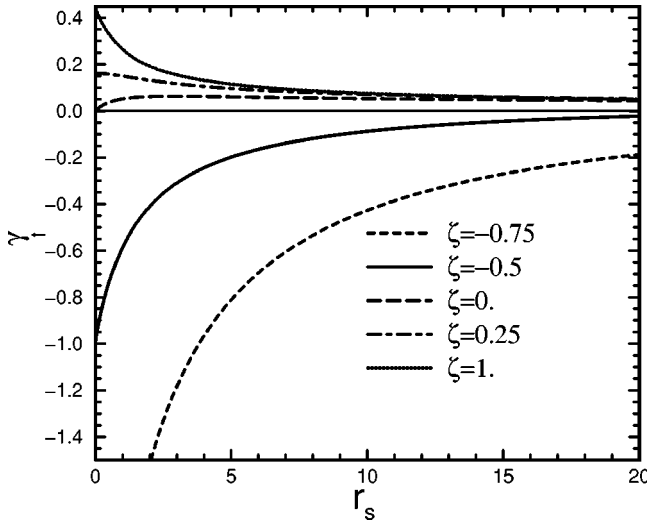


FIG. 6. The coefficient  $\gamma_1(r_s, \zeta)$  as a function of the coupling strength  $r_s$  for different values of the polarization:  $\zeta = -0.75$  (dashed curve),  $\zeta = -0.5$  (solid curve),  $\zeta = 0.0$  (long-dashed curve),  $\zeta = 0.25$  (dot-dashed curve), and  $\zeta = 1$  (dotted curve).

polarized electron gas are also computationally challenging and, so far, only results for the ground-state energy and the pair-distribution functions are available.<sup>14,32,33,15</sup>

As we have discussed in the preceding section, at small values of  $\mathbf{q}$  the local factors follow a linear dependence,  $G_\sigma^\pm(\mathbf{q} \rightarrow 0) = \alpha_\sigma^\pm(r_s, \zeta) \tilde{q}$ , where  $\tilde{q} = \mathbf{q}/k_F$ . In the opposite end of the spectrum the local corrections follow a linear plus constant dependence,  $G_\sigma^\pm(\mathbf{q} \rightarrow \infty) = \beta^\pm(r_s) + \gamma_\sigma(r_s, \zeta) \tilde{q}$ . Given the diversity of behaviors displayed by the parameters  $\alpha_\sigma^\pm$ ,  $\beta^\pm$ , and  $\gamma_\sigma$ , we will consider a general interpolating scheme for all values of  $r_s$  and  $\zeta$ . We parametrized  $G^\pm$  with two fitting parameters  $q_0^\pm$  and  $q_1^\pm$  as

$$G_\sigma^\pm(\mathbf{q}) = \alpha_\sigma^\pm \tilde{q} e^{-(\tilde{q}/q_0^\pm)^4} + (\beta^\pm + \gamma_\sigma \tilde{q}) [1 - e^{-(\tilde{q}/q_1^\pm)^4}]. \quad (13)$$

The fast decreasing exponential factors  $\exp[-(\tilde{q}/q_0^\pm)^4]$  and  $\exp[-(\tilde{q}/q_1^\pm)^4]$  are needed to mimic the rapid evolution of the local functions from their small  $\mathbf{q}$  to their large  $\mathbf{q}$  limiting behaviors. This fast evolution is clearly displayed on the latest diffusion Monte Carlo (DMC) results,<sup>11</sup> which show how the local factors  $G^+(\mathbf{q})$  and  $G^-(\mathbf{q})$  follow the predicted linear dependence at small values of the wave vector and rapidly reach their asymptotic large-wave-vector limits at not very large-values of  $\tilde{q}$ . First, we consider the parameters  $q_0^\pm$  and  $q_1^\pm$  as functions only on the electron density. By fitting Eq. (13) to the DMC results of Ref. 11 we find that the two fitting parameters are smoothly varying functions of the coupling strength and can be parametrized as

$$q_i^+ = \frac{a_i^+ + b_i^+ r_s^2}{1 + c_i^+ r_s} \quad \text{and} \quad q_i^- = \frac{a_i^- + b_i^- r_s^2}{1 + c_i^- r_s}, \quad (14)$$

where the parameters  $a_i^\pm$ ,  $b_i^\pm$ , and  $c_i^\pm$  are given in Table I. The fit for parameters  $q_i^+$  is based on DMC data of the un-

TABLE I. Optimal fit parameters for the local-field factors as parametrized in Eqs. (13) and (14).

	$i=0$	$i=1$		$i=0$	$i=1$
$a_i^+$	3.1061	2.8575	$a_i^-$	2.9432	4.3032
$b_i^+$	$6.824 \times 10^{-4}$	$1.149 \times 10^{-3}$	$b_i^-$	$1.456 \times 10^{-3}$	$8.925 \times 10^{-3}$
$c_i^+$	$5.166 \times 10^{-3}$	$3.864 \times 10^{-3}$	$c_i^-$	$3.473 \times 10^{-3}$	$4.084 \times 10^{-3}$

polarized system at  $r_s = 1, 2, 5, 10$ , and 40.<sup>11</sup> In the fit of parameters  $q_i^-$  we have to combine data of the unpolarized gas at  $r_s = 1, 2, 5$ , and 10 with data of the fully polarized system at  $r_s = 40$ . This and the fact that numerical calculations of  $G^-$  display larger error bars than the equivalent data for  $G^+$  made our parametrized expressions for  $q_i^-$  more prone to inaccuracy.

In Fig. 7 we compared our results for  $G^+(\mathbf{q})$  of the unpolarized electron gas at  $r_s = 1, 2, 5$ , and 10, Eqs. (13) and (14), with the DMC results.<sup>11</sup> In Fig. 8 our results for  $G^-(\mathbf{q})$  of the unpolarized electron gas are also compared with the numerical equivalent data. It is clear that our parametrized expressions agree very well with the quantum Monte Carlo (QMC) results.<sup>11</sup> By adding more free parameters to Eq. (13) the agreement with the numerical results will improve, but the question of how the parameters of the fit evolve with the spin polarization remains, as yet, unanswered. Thus, we keep the parametrization as simple as possible with only two free parameters.

In Fig. 9 our results for the generalized local-field correction factor  $\mathcal{G}$  of the unpolarized and fully polarized gas at  $r_s = 40$  are compared with QMC results by Moroni.<sup>34</sup> The generalized local-field function is defined as

$$\mathcal{G}(\mathbf{q}, \omega) = \frac{1}{v_{\mathbf{q}}} \left[ \frac{1}{\chi^{ee}(\mathbf{q}, \omega)} - \frac{1}{\chi^0(\mathbf{q}, \omega)} \right] + 1, \quad (15)$$

where  $\chi^{ee}$  is the charge-charge response function and  $\chi^0 = \sum_\sigma \Pi_{\sigma\sigma}$  is the Lindhard susceptibility. For the unpolarized

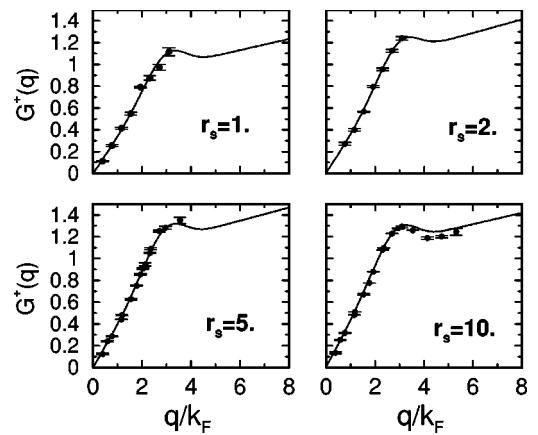


FIG. 7. Local-field correction factor  $G^+(\mathbf{q}, \omega=0)$  of the unpolarized electron gas vs normalized momentum  $\mathbf{q}/k_F$  for  $r_s = 1, 2, 5$ , and 10. The black circles correspond to the diffusion Monte Carlo (DMC) results of Ref. 11 and the solid curves are calculated according to Eqs. (13) and (14).

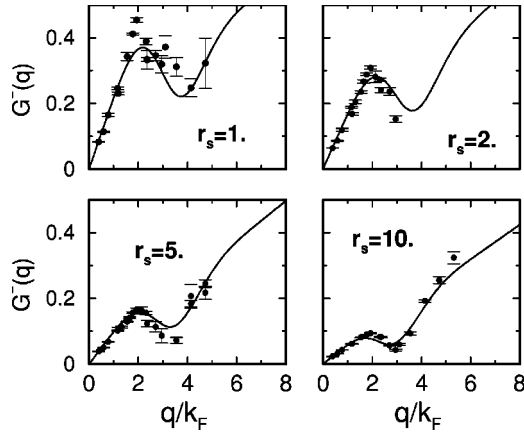


FIG. 8. Local-field correction factor  $G^-(\mathbf{q}, \omega=0)$  of the unpolarized electron gas vs normalized momentum  $\mathbf{q}/k_F$  for the same values of  $r_s$ . The black circles correspond to the DMC results of Ref. 11 and the solid curves are calculated according to Eqs. (13) and (14).

electron gas  $\mathcal{G} = G_{\uparrow}^+ = G_{\downarrow}^+$  and for a fully polarized system  $\mathcal{G} = G_{\uparrow}^+ + G_{\downarrow}^-$ . The parametrization given by Eq. (14) reproduces very well the data for the unpolarized electron gas. However, the agreement in the case of the fully polarized gas is not so good. We can closely mimic the numerical data by introducing a weak dependence of the fitting parameters  $q_i^+$  with polarization:

$$q_{0,\sigma}^+ = \frac{a_0^+ + b_0^+ r_s^2}{(1 + c_0^+ r_s)[1 + \text{sgn}(\sigma)\zeta]^{x_0}}$$

and

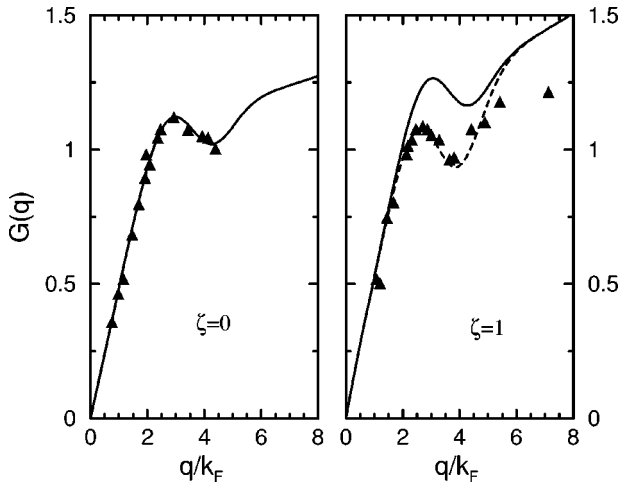


FIG. 9. Generalized local-field correction factor  $\mathcal{G}(\mathbf{q}, \omega=0)$  as defined in Eq. (15) vs normalized momentum  $\mathbf{q}/k_F$  for  $r_s=40$ . The left panel corresponds to the unpolarized system ( $\zeta=0$ ) and the right panel to the fully polarized gas ( $\zeta=1$ ). Black triangles correspond to the DMC results of Moroni (Ref. 34), solid curves are calculated according to Eqs. (13) and (14), and the dashed curve corresponds to the parameters defined in Eq. (16).

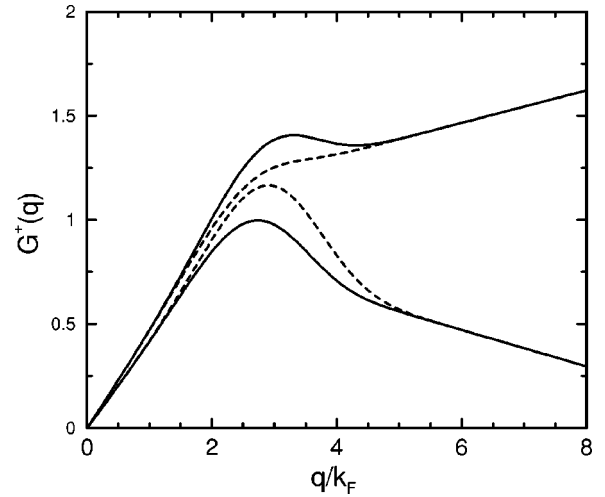


FIG. 10. Local-field corrections  $G_{\sigma}^+(\mathbf{q}, \omega=0)$  vs normalized momentum  $\mathbf{q}/k_F$  for an electron gas with  $r_s=10$  and  $\zeta=0.5$ . Upper curves correspond to  $G_{\uparrow}^+(\mathbf{q}, \omega=0)$ , lower curves to  $G_{\downarrow}^+$ . Results with nonpolarization dependence of  $q_0^+$  and  $q_1^+$  [Eq. (14)], solid curves, and with dependence on the degree of polarization [Eq. (16)], dashed curves, are included.

$$q_{1,\sigma}^+ = \frac{(a_1^+ + b_1^+ r_s^2)[1 + \text{sgn}(\sigma)\zeta]^{x_1}}{(1 + c_1^+ r_s)}, \quad (16)$$

where  $x_0=0.13076$  and  $x_1=0.035523$ . Note that this dependence with  $\zeta$  has to be considered a tentative guess since it is based only on the data at  $r_s=40$ ,  $\zeta=1$ . Figure 10 compares results for  $G_{\sigma}^+$  at  $r_s=10$  and  $\zeta=0.5$  using both parametrizations. The differences are mainly in the transition region from the small-wave-vector to the large-wave-vector behavior, where Eq. (14) generates larger values of  $G_{\uparrow}^+$  and smaller values of  $G_{\downarrow}^+$  than Eq. (16).

Using our initial parametrization scheme, Eqs. (13) and (14), we calculate the momentum dependence of the local-field functions for three values of the polarization,  $\zeta=0, 0.5$ , and  $0.9$ , and two values of the coupling strength,  $r_s=2$  (density of  $7.43 \times 10^{10} \text{ cm}^{-2}$  in GaAs) and  $r_s=10$  (density of  $0.297 \times 10^{10} \text{ cm}^{-2}$  in GaAs). Figure 11 shows our results for  $G_{\sigma}^+(\mathbf{q})$ . The factor associated with the majority spins,  $G_{\uparrow}^+$ , behaves quite different from the one of the minority spins,  $G_{\downarrow}^+$ . The field factor  $G_{\uparrow}^+$  is always positive for positive values of the polarization. It slightly increases with the degree of polarization, but it keeps the characteristic peak of the unpolarized local factor around the same value of  $\mathbf{q}$ . This peak is a residue of the sharp peak in the exchange potential,<sup>35</sup> which is washed out and/or shifted to higher values of  $\mathbf{q}$  by the inclusion of short-range correlations.<sup>36</sup> On the other hand, the behavior of  $G_{\downarrow}^+$  is dominated by the forced change in its slope, from a positive value at small  $\mathbf{q}$  to a large negative value at large wave vectors.<sup>37</sup> As a result,  $G_{\downarrow}^+$  has always a maximum, whose position shifts to lower values of  $\tilde{q}$  with increasing  $\zeta$  and it is dependent on the precise parametrization used. This issue should be explored in greater detail. Finally, Fig. 11 also compares the field factors at  $r_s=2$  and  $r_s=10$  which show similar dependence on wave vector and polarization.

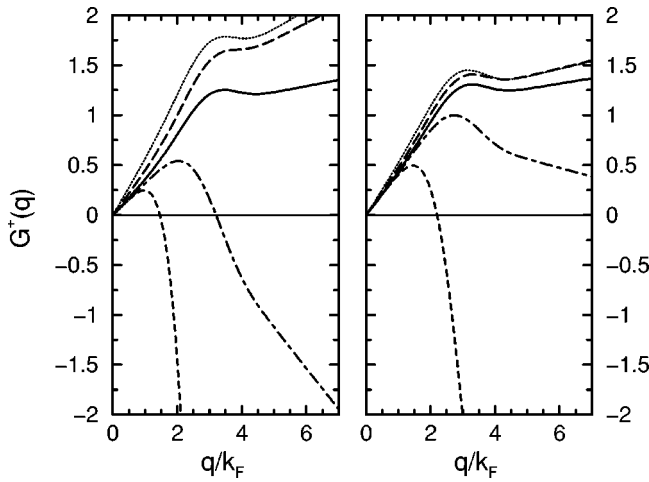


FIG. 11. Local-field corrections  $G_\sigma^+(\mathbf{q}, \omega=0)$  vs normalized momentum  $q/k_F$  for an electron gas with  $r_s=2$  (left panel) and  $r_s=10$  (right panel). Results are calculated using Eqs. (13) and (14). Results for  $G^+$  at  $\zeta=0$  (solid curves),  $G_\uparrow^+$  (long-dashed curves), and  $G_\downarrow^+$  (dot-dashed curves) at  $\zeta=0.5$ , and  $G_\uparrow^+$  (dotted curves) and  $G_\downarrow^+$  (dashed curves) at  $\zeta=0.9$  are displayed.

Figure 12 displays the local-field factor  $G_\sigma^-(\mathbf{q})$  versus normalized momentum for the same values of  $\zeta$  and  $r_s$  used in Fig. 11. The main difference between  $G_\uparrow^+(\mathbf{q})$  and  $G_\uparrow^-(\mathbf{q})$  is that the latest one displayed a sharper peak around  $\tilde{q} \sim 2$ . It appears that higher-order effects, which are important in the computation of  $G_\uparrow^+$ , cancel out in calculations of  $G_\uparrow^-$  due to the antisymmetric averaging over spin.<sup>38</sup> It is also noticeable how the local factors change with increasing  $r_s$ .

#### IV. CONCLUSIONS

We have considered an analytic parametrization of the spin-dependent local-field factors of the polarized two-dimensional electron gas, Eq. (13). Our parametrization incorporates the known asymptotic limits of the local corrections and gives an accurate fit of the available quantum Monte Carlo data.<sup>11</sup> We found that the local-field corrections associated to the minority spins strongly depend on the polarization, while the local-field functions of the majority spins are less affected by the degree of polarization. This is mainly due to the negative value of the linear term on the large  $\mathbf{q}$  limit of the local factors of the minority spins.<sup>37</sup>

The analytic parametrization used has only two parameters which have been fitted to reproduce the latest DMC results for the unpolarized and fully polarized electron gas.<sup>11</sup>

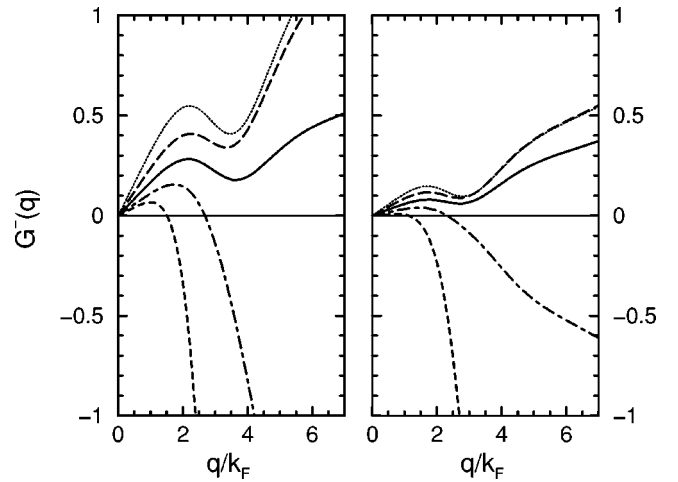


FIG. 12. Local-field corrections  $G_\sigma^-(\mathbf{q}, \omega=0)$  vs normalized momentum  $q/k_F$  for a two-dimensional electron gas with  $r_s=2$  (left panel) and  $r_s=10$  (right panel). Results are calculated using Eqs. (13) and (14). Results for  $G^-$  at  $\zeta=0$  (solid curves),  $G_\uparrow^-$  (long-dashed curves), and  $G_\downarrow^-$  (dot-dashed curves) at  $\zeta=0.5$ , and  $G_\uparrow^-$  (dotted curves) and  $G_\downarrow^-$  (dashed curves) at  $\zeta=0.9$  are included.

Since there is only a very limited set of numerically computed local-field factors, our parametrizations [Eqs. (14) and (16)] rely heavily on these results, in particular Eq. (16) which includes a dependence on polarization. Therefore, further study will be needed to evaluate the efficacy of our parametrization and their precise dependence on the spin polarization and density.

In conclusion, we believe that our approach provides a realistic qualitative description of the paramagnetic phase of the polarized electron gas. Caution, however, should be exercised in applying our calculation in the limit of  $\zeta$  approaching unity, where the paramagnetic model breaks down. We have found that for small values of  $r_s$ , the magnetic susceptibility and the inverse dielectric constant develop a pole at the same value of the electronic density and spin polarization. This fact signals a charge-spin density wave instability in the polarized electron gas and it will be discussed elsewhere.<sup>39</sup>

#### ACKNOWLEDGMENTS

We thank S. Moroni for enlightened discussions and to him and G. Senatore for providing us with the results of their numerical calculation of the local-field factors. We gratefully acknowledge the financial support provided by the U.S. Department of Energy, Grant No. DE-FG02-01ER45897.

<sup>1</sup>S.A. Crooker, D.A. Tulchinsky, J. Levy, D.D. Awschalom, R. Garcia, and N. Samarth, Phys. Rev. Lett. **75**, 505 (1995).

<sup>2</sup>For a review, see G. Prinz and K. Hathaway, Phys. Today **48**(4), 24 (1995).

<sup>3</sup>G.D. Mahan, *Many-Particle Physics* (Plenum Press, New York, 1990), Chap. 5.

<sup>4</sup>C.A. Kukkonen and A.W. Overhauser, Phys. Rev. B **20**, 550 (1979).

<sup>5</sup>X. Zhu and A.W. Overhauser, Phys. Rev. B **33**, 925 (1986).

<sup>6</sup>K.S. Yi and J. J. Quinn, Phys. Rev. B **54**, 13 398 (1996).

<sup>7</sup>D.C. Marinescu and J.J. Quinn, Phys. Rev. B **56**, 1114 (1997).

<sup>8</sup>C.F. Richardson and N.W. Ashcroft, Phys. Rev. B **50**, 8170 (1994); **55**, 15 130 (1997).

<sup>9</sup>D.C. Marinescu and I. Tifrea, Phys. Rev. B **65**, 113201 (2002).

<sup>10</sup>M. Polini and M.P. Tosi, Phys. Rev. B **63**, 045118 (2001).

<sup>11</sup>S. Moroni, D.M. Ceperley, and G. Senatore, Phys. Rev. Lett. **69**,

- 1837 (1992); **75**, 689 (1995); G. Senatore, S. Moroni, and D.M. Ceperley, in *Quantum Monte Carlo Methods in Physics and Chemistry*, edited by M.P. Nightingale and C.J. Umrigar (Kluwer Academic, Dordrecht, 1999); G. Senatore, S. Moroni, and D. Varsano, *Solid State Commun.* **119**, 333 (2001); (private communication).
- <sup>12</sup>  $a_B^*$  is the effective Bohr radius of the system,  $a_B^* = \hbar^2 / (m^* e^2)$ . For a regular three-dimensional metal  $a_B^* = a_0 = 0.529 \times 10^{-8}$  cm and  $a_B^* = 195a_0 = 1.04 \times 10^{-6}$  cm for GaAs.
- <sup>13</sup> The dielectric function also develops a pole at the same value of the coupling strength. However, a pole in the dielectric function indicates not an instability of the paramagnetic phase but a region in momentum space where the Coulomb interaction is over-screened. See O.V. Dolgov, D.A. Kirzhnits, and E.G. Maksimov, *Rev. Mod. Phys.* **53**, 81 (1981) and references therein.
- <sup>14</sup> B. Tanatar and D.M. Ceperley, *Phys. Rev. B* **39**, 5005 (1989).
- <sup>15</sup> C. Attaccalite, S. Moroni, P. Gori-Giorgi, and G.B. Bachelet, *Phys. Rev. Lett.* **88**, 256601 (2002).
- <sup>16</sup> The quenching of the divergence at  $\zeta \pm 1$  will depend on the precise parametrization used for the correlation energy.
- <sup>17</sup> G. Niklasson, *Phys. Rev. B* **10**, 3052 (1974).
- <sup>18</sup> M. Polini, G. Sica, B. Davoudi, and M.P. Tosi, *J. Phys.: Condens. Matter* **13**, 3591 (2001).
- <sup>19</sup> J. Moreno and D.C. Marinescu, *J. Phys.: Condens. Matter* **15**, 6321 (2003).
- <sup>20</sup> A. Holas, in *Strongly Coupled Plasma Physics*, edited by F.J. Rogers and H.E. DeWitt (Plenum, New York, 1987), p. 463.
- <sup>21</sup> B. Davoudi, M. Polini, G.F. Giuliani, and M.P. Tosi, *Phys. Rev. B* **64**, 153101 (2001); **64**, 233110 (2001).
- <sup>22</sup> G.F. Giuliani and G. Vignale, *Quantum Theory of the Electron Liquid*, (Cambridge University Press, Cambridge, in press).
- <sup>23</sup> J. Moreno (unpublished).
- <sup>24</sup> J.P. Perdew and Y. Wang, *Phys. Rev. B* **45**, 13244 (1992).
- <sup>25</sup> A.W. Overhauser, *Phys. Rev. B* **4**, 3318 (1971).
- <sup>26</sup> K.S. Singwi, A. Sjölander, M.P. Tosi, and R.H. Land, *Phys. Rev. B* **1**, 1044 (1970).
- <sup>27</sup> P. Vashishta and K.S. Singwi, *Phys. Rev. B* **6**, 875 (1972).
- <sup>28</sup> M. Corradini, R. Del Sole, G. Onida, and M. Palumbo, *Phys. Rev. B* **57**, 14 569 (1998).
- <sup>29</sup> N. Iwamoto, *Phys. Rev. B* **43**, 2174 (1991).
- <sup>30</sup> C. Bulutay and M. Tomak, *Phys. Rev. B* **53**, 7317 (1996).
- <sup>31</sup> J. Hubbard, *Proc. R. Soc. London, Ser. A* **240**, 539 (1957); **243**, 336 (1957).
- <sup>32</sup> C. Bulutay and B. Tanatar, *Phys. Rev. B* **65**, 195116 (2002).
- <sup>33</sup> B. Davoudi and M.P. Tosi, cond-mat/0107519 (unpublished).
- <sup>34</sup> Results from S. Moroni as included in V. Tozzini and M.P. Tosi, *J. Phys.: Condens. Matter* **8**, 8121 (1996).
- <sup>35</sup> Y.R. Wang, M. Ashraf and A.W. Overhauser, *Phys. Rev. B* **30**, 5580 (1984).
- <sup>36</sup> F. Pederiva, E. Lipparini, and K. Takayanagi, *Europhys. Lett.* **40**, 607 (1997).
- <sup>37</sup> The negative slope of  $G^\pm$  for minority spins is a result of the fact that electrons from the majority-spin population tend to accumulate around the few minority spins. Also, since
- $$G_\sigma^n(q \rightarrow \infty) = \frac{1}{2v(q)} \left[ \frac{1}{\Pi_{\sigma,\sigma}} - \frac{1}{\Pi_{\sigma,\sigma}^0} \right] \sim \frac{1}{n_\sigma^2},$$
- the slope of  $G^\pm$  diverges faster for minority spins.
- <sup>38</sup> G.S. Atwal and N.W. Ashcroft, *Phys. Rev. B* **67**, 115107 (2003).
- <sup>39</sup> J. Moreno and D.C. Marinescu (unpublished).